

This is a copy of the published version, or version of record, available on the publisher's website. This version does not track changes, errata, or withdrawals on the publisher's site.

## Sensors and actuators for the advanced LIGO A+ upgrade

S. J. Cooper, C. M. Mow-Lowry, D. Hoyland, J. Bryant, A. Ubhi, J. O'Dell, A. Huddart, S. Aston, and A. Vecchio

### Published version information

**Citation:** SJ Cooper et al. Sensors and actuators for the advanced LIGO A+ upgrade. Rev Sci Instrum 94, no. 1 (2023): 014502

**DOI:** [10.1063/5.0117605](https://doi.org/10.1063/5.0117605)

This article may be downloaded for personal use only. Any other use requires prior permission of the author and AIP Publishing. This article appeared as cited above.

This version is made available in accordance with publisher policies. Please cite only the published version using the reference above. This is the citation assigned by the publisher at the time of issuing the APV. Please check the publisher's website for any updates.

This item was retrieved from **ePubs**, the Open Access archive of the Science and Technology Facilities Council, UK. Please contact [epublications@stfc.ac.uk](mailto:epublications@stfc.ac.uk) or go to <http://epubs.stfc.ac.uk/> for further information and policies.

# Sensors and actuators for the advanced LIGO A+ upgrade

Cite as: Rev. Sci. Instrum. **94**, 014502 (2023); <https://doi.org/10.1063/5.0117605>

Submitted: 01 August 2022 • Accepted: 21 December 2022 • Published Online: 10 January 2023

 S. J. Cooper,  C. M. Mow-Lowry,  D. Hoyland, et al.



View Online



Export Citation



CrossMark

## ARTICLES YOU MAY BE INTERESTED IN

[An ultra-high vacuum system for fabricating clean two-dimensional material devices](#)



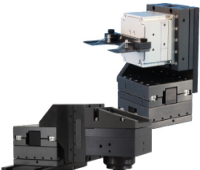
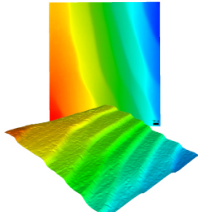
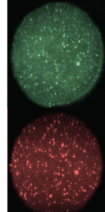
Review of Scientific Instruments **94**, 013903 (2023); <https://doi.org/10.1063/5.0110875>

[Feasibility of seismic wave communication using electromagnetic vibrator under strong environmental noise interference: Field experimental research](#)

Review of Scientific Instruments **94**, 014503 (2023); <https://doi.org/10.1063/5.0116657>

[A VME: Versa Module Europa, crate controller for high speed data acquisition of heterogeneous, multi-detector systems](#)

Review of Scientific Instruments **94**, 013304 (2023); <https://doi.org/10.1063/5.0107168>

|                                                                                                                                                                                         |                                                                                                                    |                                                                                                                    |                                                                                                                       |                                                                                                                          |
|-----------------------------------------------------------------------------------------------------------------------------------------------------------------------------------------|--------------------------------------------------------------------------------------------------------------------|--------------------------------------------------------------------------------------------------------------------|-----------------------------------------------------------------------------------------------------------------------|--------------------------------------------------------------------------------------------------------------------------|
| <br><b>MCL</b><br>MAD CITY LABS INC.<br><a href="http://www.madcitylabs.com">www.madcitylabs.com</a> | <p>Nanopositioning Systems</p>  | <p>Modular Motion Control</p>  | <p>AFM and NSOM Instruments</p>  | <p>Single Molecule Microscopes</p>  |
|-----------------------------------------------------------------------------------------------------------------------------------------------------------------------------------------|--------------------------------------------------------------------------------------------------------------------|--------------------------------------------------------------------------------------------------------------------|-----------------------------------------------------------------------------------------------------------------------|--------------------------------------------------------------------------------------------------------------------------|

# Sensors and actuators for the advanced LIGO A+ upgrade

Cite as: Rev. Sci. Instrum. 94, 014502 (2023); doi: 10.1063/5.0117605

Submitted: 1 August 2022 • Accepted: 21 December 2022 •

Published Online: 10 January 2023



View Online



Export Citation



CrossMark

S. J. Cooper,<sup>1</sup>  C. M. Mow-Lowry,<sup>1,a)</sup>  D. Hoyland,<sup>1</sup>  J. Bryant,<sup>1</sup> A. Ubhi,<sup>1</sup>  J. O'Dell,<sup>2</sup> A. Huddart,<sup>2</sup>  
S. Aston,<sup>3</sup>  and A. Vecchio<sup>1</sup> 

## AFFILIATIONS

<sup>1</sup>Institute for Gravitational Wave Astronomy and School of Physics and Astronomy, University of Birmingham, Birmingham B15 2TT, United Kingdom

<sup>2</sup>Science and Technology Facilities Council, Rutherford Appleton Laboratory, Harwell Campus, Didcot OX11 0QX, United Kingdom

<sup>3</sup>LIGO Livingston Observatory, Livingston, Louisiana 70754, USA

<sup>a)</sup>Author to whom correspondence should be addressed: [conor.mow-lowry@ligo.org](mailto:conor.mow-lowry@ligo.org)

## ABSTRACT

Advanced Laser Interferometer Gravitational-wave Observatory (LIGO A+) is a major upgrade to LIGO—the Laser Interferometer Gravitational-wave Observatory. For the A+ project, we have developed, produced, and *characterized* sensors and electronics to interrogate new optical suspensions designed to isolate optics from vibrations. The central element is a displacement sensor with an integrated electromagnetic actuator known as a BOSEM (Birmingham Optical Sensor and ElectroMagnetic actuator) and its readout and drive electronics required to integrate them into LIGO's control and data system. In this paper, we report on the improvements to the sensors and the testing procedures undertaken to meet the enhanced performance requirements set out by the A+ upgrade to the detectors. The best devices reach a noise level of  $4.5 \times 10^{-11}$  m/ $\sqrt{\text{Hz}}$  at a measurement frequency of 1 Hz, an improvement of 6.7 times over standard devices.

Published under an exclusive license by AIP Publishing. <https://doi.org/10.1063/5.0117605>

## I. INTRODUCTION

The advanced Laser Interferometer Gravitational-wave Observatory (LIGO)<sup>1</sup> and Virgo<sup>2</sup> gravitational-wave interferometers have opened up the explorations of the gravitational-wave sky, with the observation of the coalescence of stellar-mass binary black holes,<sup>3–8</sup> binary neutron stars,<sup>9–11</sup> and more recently, neutron star–black hole systems.<sup>12</sup>

The LIGO (Laser Interferometer and Gravitational-wave Observatory) and Virgo detectors are being upgraded to what is known as the “Advanced+” (A+, hereafter) configuration. The installation has already begun for some of the hardware. After the fourth observing run (O4) scheduled to start in March 2023, it will be completed in advance of the fifth observing run in 2025.<sup>13</sup> The higher sensitivity achieved through this upgrade will correspond to an increase in the Universe's observable volume by a factor  $\approx 5$  with respect to the one probed by the existing instruments, resulting in an equal increase in the detection rate. For example, based

on the current estimates of the merger rate of populations of stellar-mass binary systems<sup>14</sup> and the expected instrument performance in A+ configurations, the detectors will observe several of such binary coalescences every week.<sup>15</sup>

LIGO A+ will achieve this increase in the observing range by upgrading several subsystems of the detectors: new test-masses with reduced coating thermal noise,<sup>16</sup> frequency-dependent squeezing,<sup>17</sup> replacement of the central beam-splitter with a larger optic, and installation of balanced homodyne detection<sup>18</sup> to further reduce quantum noise.

These upgrades will require several new multi-stage suspension systems for isolating and controlling the new optical elements. Each suspension requires a set of low-noise sensors and actuators, with associated electronics, to actively damp resonances and steer the laser beam. One example of a new suspension, shown in Fig. 1, is the “HAM Relay Triple Suspension,” an evolution of the existing suspension designs that is lighter and easier to assemble. In total, 200 BOSEMs—“Birmingham Optical Sensor and ElectroMagnetic

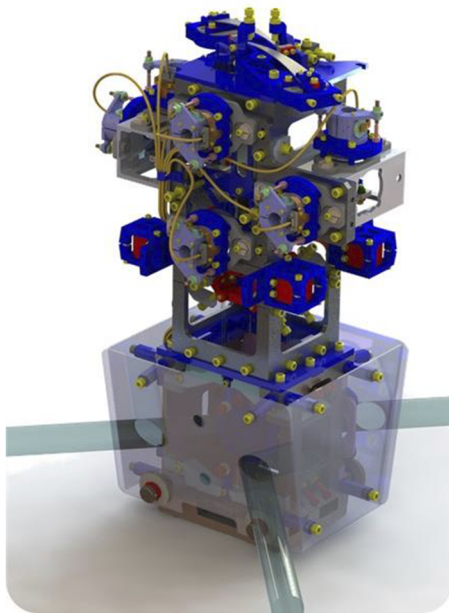


**FIG. 1.** A rendered image of the new HAM Relay Triple Suspension with BOSEMs installed. Six BOSEMs are connected to yellow cables in the upper part of the suspension.

actuators”—have been produced, along with 82 coil-driver units and 44 “satellite amplifiers” for reading out the photocurrent.

This paper updates the design produced for the advanced LIGO<sup>19,20</sup> to fulfill the existing and enhanced sensitivity requirements for A+. A noise budget with the dominant terms is provided, with reference to the exhaustive selection procedure required. More than half of the BOSEMs reach a new “enhanced” performance requirement. The best enhanced BOSEMs are now dominated by quantum shot noise across the whole measurement band from 50 mHz to 20 Hz, a major performance improvement. The effect of the improved sensor noise is non-trivial to estimate. A case study using interferometric “HoQI” (Homodyne Quadrature Interferometer) sensors on the new bigger beam splitter suspension for LIGO describes the process for determining the performance.<sup>21,22</sup>

## II. BOSEM DESIGN

BOSEMs are compact, ultra-high vacuum compliant, non-contact, and low-noise position sensors with integrated electromagnetic actuators. They have a long history of development started by studies on the initial LIGO OSEMs by Fritschel and Adhikari,<sup>23</sup> which were upgraded to AOSEMs by Abbott *et al.*<sup>24</sup> and modified by Carbone *et al.*<sup>19</sup> to produce the advanced LIGO BOSEMs. The key parameters for each BOSEM are shown in Table I.

Each BOSEM unit comprises of a number of elements: sensing, actuation, and alignment. An exploded computer aided design (CAD) model of a BOSEM is shown in Fig. 2, with the key features of the sensor labeled. The optical readout is based on a shadow sensing scheme where an opaque “flag,” rigidly mounted to the measurement surface,<sup>25</sup> partly blocks the 935 nm light emitted from an

**TABLE I.** Key parameters for a BOSEM.

| Parameter                              | Value                                                                |
|----------------------------------------|----------------------------------------------------------------------|
| Coil                                   |                                                                      |
| Turns                                  | 800                                                                  |
| Winding sense                          | Clockwise when viewed from the rear face                             |
| Inductance                             | $14.7 \pm 0.7$ mH                                                    |
| Resistance                             | $37.6 \pm 2$ $\Omega$                                                |
| Length                                 | 8 mm                                                                 |
| Inner coil diameter                    | 17.8 mm                                                              |
| Maximum current                        | 150 mA                                                               |
| Breakdown (to coil former)             | >200 V                                                               |
| Sensor                                 |                                                                      |
| Total mass                             | 158 g                                                                |
| Linear range (typ.)                    | 0.7 mm                                                               |
| Operating LED current                  | 35 mA                                                                |
| Photodiode bias                        | 10 V typ. (50 V max.)                                                |
| Photocurrent, open-light               | 45–80 $\mu$ A                                                        |
| Current transfer ratio                 | $0.19\% \pm 0.04\%$                                                  |
| Average sensitivity                    | 20.25 kV/m                                                           |
| Electrical connector                   | Glenair Micro-D<br>MR7590-9P-1BSN-MC225                              |
| Mechanical interface                   | 4 $\times$ 8/32UNC thru-holes on a<br>40.64 mm (1.3 in.) square grid |
| Operating temperature                  | $22 \pm 2$ $^{\circ}$ C                                              |
| Storage temperature (ambient pressure) | 10–120 $^{\circ}$ C                                                  |
| Sensor noise                           |                                                                      |
| Standard                               |                                                                      |
| 1–10 Hz                                | $3 \times 10^{-10}$ m/ $\sqrt{\text{Hz}}$                            |
| 10–20 Hz                               | $1 \times 10^{-10}$ m/ $\sqrt{\text{Hz}}$                            |
| Enhanced                               |                                                                      |
| 1–20 Hz                                | $<0.75 \times 10^{-10}$ m/ $\sqrt{\text{Hz}}$                        |

infrared LED (IRLED, Optek OP132) before it is sensed by a photodiode (PD, Osram BPX 65). The choice of wavelength ensures a high quantum efficiency from the silicon photodiode and a negligible emission at 1064 nm, the wavelength of the main science laser. A lens is installed after the LED to produce a narrower beam and smaller spot on the photodiode, improving both the linearity and sensitivity of the BOSEM.

To meet the LIGO’s stringent vacuum requirements, the BOSEMs must go through a multi-stage cleaning process. In the original production run, toluene was used in the cleaning process to remove paraffin from the coil wire.<sup>26</sup> Following the detection of toluene residue in RGA scans during the production process, the coil wire was switched (from MWS Wire 32 HML to MWS Wire 32 HML Natural) to ensure that the production process was paraffin-free. The updated cleaning process can be found in Ref. 27.

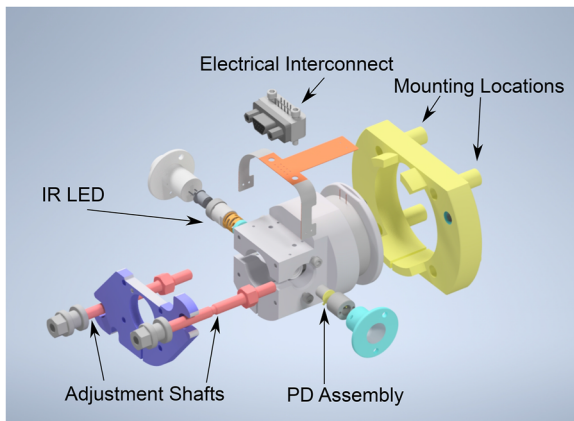


FIG. 2. An exploded view of a BOSEM highlighting the key components.

### III. PERFORMANCE ANALYSIS

The noise budget of a BOSEM is shown in Fig. 3. The noise sources expected to dominate a typical system are the shot noise and the photodiode dark noise. The shot noise, shown in dark blue, is modeled and projected to an equivalent displacement using

$$SN = \frac{2R}{K} \sqrt{2eI}, \quad (1)$$

where  $e$  is the electronic charge,  $I$  is the photocurrent at the operating point (the “half-light” current),  $R$  is the transimpedance gain of 121 kΩ, and  $K$  is the sensitivity of the BOSEM, which varies depending on the photocurrent but averages 20 250 V per meter. The leading factor of two accounts for the differential output gain of the satellite amplifier. The photodiode dark noise, shown in red, was measured by switching off the IRLED and measuring the output of the satellite amplifier.<sup>19</sup>

The total modeled noise trace, shown in purple, is achieved by summing the shot noise and dark noise in quadrature. This noise

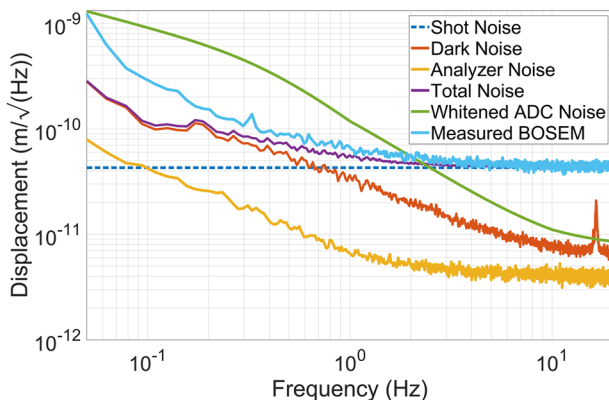


FIG. 3. A noise budget of an enhanced BOSEM showing each of the individual noise contributions. The main noise sources are the shot noise (dashed dark blue) and the photodiode dark noise (red). The resolution of the BOSEM at the critical 10 Hz measurement frequency is limited by optical shot noise.

model is compared with the spectrum of a typical BOSEM “open light test,” where there is no flag inserted in the beam, shown in light blue. Since the open light test has a factor of two more photocurrent than the normal half-light operation, to calibrate it into meters, we divide by a factor of  $\sqrt{2}$  before using the volts-to-meters conversion factor. This will correctly scale the shot-noise for the photocurrent expected under normal operating conditions.

The noise floor of our signal analyzer is shown for reference in yellow. The whitenized analog-to-digital converter (ADC) noise of LIGO’s control and data system is shown in green; at frequencies lower than 2 Hz, we expect the BOSEMs installed at LIGO to be dominated by this noise source.

There is a clear discrepancy between the noise model and the measurement of a typical BOSEM. Two contributions have been identified. First, the photodiode dark noise varies from unit to unit, presumably due to defects in individual photodiodes. Repeated measurements have shown that this never exceeds the noise requirements and is sub-dominant in almost all BOSEM assemblies. Second, the IRLEDs show a significant, excess intensity fluctuation and this is the dominant source of excess noise. This excess noise was identified in the original advanced LIGO BOSEM production run, and a screening process was implemented to select IRLEDs that comply with the noise requirements.<sup>28</sup> For the A+ upgrade, we conducted an extensive review of different IRLEDs, but no model was shown to consistently meet the noise requirements. Instead, the advanced LIGO screening process was improved, most importantly by lengthening the initial “burn in” from 50 to 168 h, as detailed in Ref. 29.

To capitalize on the effort involved in screening every IRLED, we identified units with an especially good noise performance between 1 and 20 Hz. If these units met a new “enhanced” noise requirement, they were separated and tagged for use in critical locations. They do not require any change to the existing signal chain. Figure 4 shows the noise spectra of a standard BOSEM and an enhanced BOSEM, along with their respective requirements. The best of the enhanced BOSEMs are dominated by shot noise across the whole measurement band. Further improvements can come

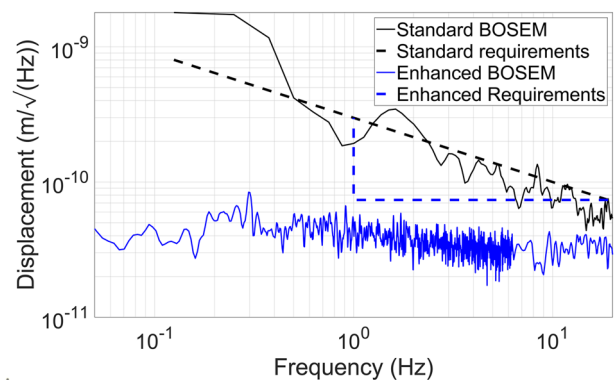


FIG. 4. Amplitude spectral density of a standard (black) and an enhanced (blue) BOSEM compared against the noise requirements shown with dashed lines.

from reducing the measurement range (increasing the sensitivity), for example by using differential-OSEMs<sup>30</sup> or an alternative technology such as fringe-counting interferometers,<sup>21</sup> which have an improved resolution without sacrificing the operating range.

#### IV. CONCLUSIONS

As part of the LIGO A+ upgrade, the University of Birmingham has provided over 200 BOSEMs along with their associated driving electronics. Over half of the BOSEMs meet the “enhanced” specifications. The best units have a resolution of  $4.5 \times 10^{-11} \text{ m}/\sqrt{\text{Hz}}$ , all the way down to 0.1 Hz, and these devices represent the ultimate performance of BOSEMs in their current form.

#### ACKNOWLEDGMENTS

We thank Jeff Kissel for his useful comments on the manuscript. This work was supported by the UK’s Science and Technology Facilities Council through Grant No. ST/S00243X/1. A.V. acknowledges the support of the Royal Society and Wolfson Foundation. The authors gratefully acknowledge the support of the United States NSF for the construction and operation of the LIGO Laboratory and Advanced LIGO. LIGO was constructed by the California Institute of Technology and Massachusetts Institute of Technology with the funding from the United States National Science Foundation (NSF) and operates under Cooperative Agreement No. PHY-1764464. The Advanced LIGO was built under Award No. PHY-0823459.

#### AUTHOR DECLARATIONS

##### Conflict of Interest

The authors have no conflicts to disclose.

##### Author Contributions

**S. J. Cooper:** Supervision (equal); Writing – original draft (lead); Writing – review & editing (equal). **C. M. Mow-Lowry:** Supervision (equal); Writing – original draft (equal); Writing – review & editing (equal). **D. Hoyland:** Investigation (equal); Methodology (equal); Writing – original draft (equal); Writing – review & editing (equal). **J. Bryant:** Investigation (equal); Methodology (equal). **A. Ubhi:** Investigation (equal); Methodology (equal). **J. O’Dell:** Resources (equal). **A. Huddart:** Resources (equal). **S. Aston:** Methodology (equal). **A. Vecchio:** Investigation (equal); Writing – original draft (equal); Writing – review & editing (equal).

#### DATA AVAILABILITY

Data and models used to produce Figs. 3 and 4 are available on request.

#### REFERENCES

- <sup>1</sup>A. Buikema *et al.*, “Sensitivity and performance of the Advanced LIGO detectors in the third observing run,” *Phys. Rev. D* **102**, 062003 (2020).
- <sup>2</sup>F. Acernese, M. Agathos, A. Ain, S. Albanesi, A. Allocca, A. Amato, T. Andrade, N. Andres, T. Andrić, S. Ansoldi *et al.*, “Calibration of Advanced Virgo and

reconstruction of detector strain  $h(t)$  during the observing run O3,” [arXiv:2107.03294](https://arxiv.org/abs/2107.03294) (2021).

- <sup>3</sup>B. P. Abbott *et al.*, “Observation of gravitational waves from a binary black hole merger,” *Phys. Rev. Lett.* **116**(6), 061102 (2016).
- <sup>4</sup>B. P. Abbott *et al.*, “Binary black hole mergers in the first Advanced LIGO observing run,” *Phys. Rev. X* **6**(4), 041015 (2016); Erratum **8**, 039903 (2018).
- <sup>5</sup>B. P. Abbott *et al.*, “GWTC-1: A gravitational-wave transient catalog of compact binary mergers observed by LIGO and Virgo during the first and second observing runs,” *Phys. Rev. X* **9**(3), 031040 (2019).
- <sup>6</sup>R. Abbott *et al.*, “GWTC-2: Compact binary coalescences observed by LIGO and Virgo during the first half of the third observing run,” *Phys. Rev. X* **11**, 021053 (2021).
- <sup>7</sup>R. Abbott *et al.*, “GWTC-2.1: Deep extended catalog of compact binary coalescences observed by LIGO and Virgo during the first half of the third observing run,” [arXiv:2108.01045](https://arxiv.org/abs/2108.01045) (2021).
- <sup>8</sup>R. Abbott *et al.*, “GWTC-3: Compact binary coalescences observed by LIGO and Virgo during the second part of the third observing run,” [arXiv:2111.03606](https://arxiv.org/abs/2111.03606) (2021).
- <sup>9</sup>B. P. Abbott *et al.*, “GW170817: Observation of gravitational waves from a binary neutron star inspiral,” *Phys. Rev. Lett.* **119**(16), 161101 (2017).
- <sup>10</sup>B. P. Abbott *et al.*, “Multi-messenger observations of a binary neutron star merger,” *Astrophys. J. Lett.* **848**(2), L12 (2017).
- <sup>11</sup>B. P. Abbott *et al.*, “GW190425: Observation of a compact binary coalescence with total mass  $\sim 3.4M_{\odot}$ ,” *Astrophys. J. Lett.* **892**, L3 (2020).
- <sup>12</sup>R. Abbott *et al.*, “Observation of gravitational waves from two neutron star-black hole coalescences,” *Astrophys. J. Lett.* **915**, L5 (2021).
- <sup>13</sup>B. P. Abbott, R. Abbott, T. D. Abbott *et al.*, “Prospects for observing and localizing gravitational-wave transients with Advanced LIGO, Advanced Virgo and KAGRA,” *Living Rev. Relativ.* **23**, 3 (2020).
- <sup>14</sup>R. Abbott *et al.*, “The population of merging compact binaries inferred using gravitational waves through GWTC-3,” [arXiv:2111.03634](https://arxiv.org/abs/2111.03634) (2021).
- <sup>15</sup>The Virgo Collaboration, Advanced Virgo Plus Phase I-Design Report No. VIR-0596A-19, Virgo Technical Documentation System, 2019, available at <https://tds.virgo-gw.eu/ql/?c=14430>.
- <sup>16</sup>G. Vajente, L. Yang, A. Davenport, M. Fazio, A. Ananyeva, L. Zhang, G. Billingsley, K. Prasai, A. Markosyan, R. Bassiri, M. M. Fejer, M. Chicoine, F. Schiettekatte, and C. S. Menoni, “Low mechanical loss  $\text{TiO}_2$ :  $\text{GeO}_2$  coatings for reduced thermal noise in gravitational wave interferometers,” *Phys. Rev. Lett.* **127**, 071101 (2021).
- <sup>17</sup>L. McCuller, C. Whittle, D. Ganapathy, K. Komori, M. Tse, A. Fernandez-Galiana, L. Barsotti, P. Fritschel, M. MacInnis, F. Matichard, K. Mason, N. Mavalvala, R. Mittleman, H. Yu, M. E. Zucker, and M. Evans, “Frequency-dependent squeezing for advanced LIGO,” *Phys. Rev. Lett.* **124**, 171102 (2020).
- <sup>18</sup>P. Fritschel, M. Evans, and V. Frolov, “Balanced homodyne readout for quantum limited gravitational wave detectors,” *Opt. Express* **22**, 4224–4234 (2014).
- <sup>19</sup>L. Carbone, S. M. Aston, R. M. Cutler, A. Freise, J. Greenhalgh, J. Heefner, D. Hoyland, N. A. Lockerbie, D. Lodhia, N. A. Robertson, C. C. Speake, K. A. Strain, and A. Vecchio, “Sensors and actuators for the Advanced LIGO mirror suspensions,” *Classical Quantum Gravity* **29**, 115005 (2012).
- <sup>20</sup>S. M. Aston, M. A. Barton, A. S. Bell, N. Beveridge, B. Bland, A. J. Brummitt, G. Cagnoli, C. A. Cantley, L. Carbone, A. V. Cumming, L. Cunningham, R. M. Cutler, R. J. S. Greenhalgh, G. D. Hammond, K. Haughian, T. M. Hayler, A. Heptonstall, J. Heefner, D. Hoyland, J. Hough, R. Jones, J. S. Kissel, R. Kumar, N. A. Lockerbie, D. Lodhia, I. W. Martin, P. G. Murray, J. O’Dell, M. V. Plissi, S. Reid, J. Romie, N. A. Robertson, S. Rowan, B. Shapiro, C. C. Speake, K. A. Strain, K. V. Tokmakov, C. Torrie, A. A. van Veggel, A. Vecchio, and I. Wilmot, “Update on quadruple suspension design for Advanced LIGO,” *Classical Quantum Gravity* **29**, 235004 (2012).
- <sup>21</sup>S. J. Cooper, C. J. Collins, A. C. Green, D. Hoyland, C. C. Speake, A. Freise, and C. M. Mow-Lowry, “A compact, large-range interferometer for precision measurement and inertial sensing,” *Classical Quantum Gravity* **35**, 095007 (2018).

- <sup>22</sup>J. van Dongen, L. Prokhorov, S. J. Cooper, M. A. Barton, E. Bonilla, K. L. Dooley, J. C. Driggers, A. Effler, N. A. Holland, A. Huddart, M. Kasprzack, J. S. Kissel, B. Lantz, A. L. Mitchell, J. O'Dell, A. Pele, C. Robertson, and C. M. Mow-Lowry, "Reducing controls noise in gravitational wave detectors with interferometric local damping of suspended optics," *arXiv:2205.01434* (2022).
- <sup>23</sup>P. Fritschel and R. Adhikari, Characterization and comparison of a potential new (SUS) local sensor, LIGO Document Control Center, available at <https://dcc.ligo.org/LIGO-T990089/public>, 2015.
- <sup>24</sup>R. Abbott, M. Barton, B. Bland, B. Moore, C. Osthelder, and J. Romie, Advanced LIGO OSEM final design document, LIGO Document Control Center, available at <https://dcc.ligo.org/LIGO-T0900286/public>, 2014.
- <sup>25</sup>M. Evans and M. Hillard, BOSEM flat magnet flag, aLIGO SUS, LIGO Document Control Center, available at <https://dcc.ligo.org/LIGO-D1100573/public>, 2011.
- <sup>26</sup>C. Taylor, Cleaning procedure for magnet wire with ML/HML insulation, LIGO Document Control Center, available at <https://dcc.ligo.org/T040127>, 2019.
- <sup>27</sup>J. L. Bryant, S. M. Aston, D. Lodhia, and D. Hoyland, BOSEM assembly specification, LIGO Document Control Center, available at <https://dcc.ligo.org/LIGO-T060233/public>, 2021.
- <sup>28</sup>S. M. Aston, "Optical read-out techniques for the control of test-masses in gravitational wave observatories," Ph.D. thesis (University of Birmingham, 2011), available at <https://etheses.bham.ac.uk/id/eprint/1665/>.
- <sup>29</sup>D. Hoyland and J. L. Bryant, A+ BOSEM IR-LED screening, LIGO Document Control Center, available at <https://dcc.ligo.org/LIGO-T1900596/public>, 2019.
- <sup>30</sup>J. Conklin, D. Jariwala, T. Pechsiri, H. Inchauspe, P. Fulda, and D. Tanner, Progress in developing a differential OSEM (DOSEM), LIGO Document Control Center, available at <https://dcc.ligo.org/LIGO-G1900464>, 2019.